

# Role of Endothelin-1 in the Migration of Human Olfactory Gonadotropin-Releasing Hormone-Secreting Neuroblasts

Roberto G. Romanelli, Tullio Barni, Mario Maggi, Michaela Luconi, Paola Failli, Anna Pezzatini, Annamaria Morelli, Roberto Maggi, Roberta Zaninetti, Roberto Salerno, Stefano Ambrosini, Mirca Marini, Carlo M. Rotella, and Gabriella B. Vannelli

*Departments of Anatomy Histology and Forensic Medicine (A.P., S.A., M.M., G.B.V.), Clinical Physiopathology and Endocrinology (R.S., C.M.R.), and Andrology Units (M.M., M.L., A.M.), Internal Medicine (R.G.R.), and Preclinical and Clinical Pharmacology (P.F.), University of Florence, I-50134 Florence; Department of Endocrinology (R.M., R.Z.), University of Milan, 20133 Milan; and Experimental and Clinical Medicine (T.B.), University of Catanzaro, 88100 Catanzaro, Italy*

**FNC-B4 neuroblasts that express both neuronal and olfactory markers have been established and cloned. These cells express GnRH and both the endothelin-1 (ET-1) gene and protein and respond in a migratory manner to GnRH in a dose-dependent manner. Previous research has shown that FNC-B4 cells produce and respond to ET-1 by regulating the secretion of GnRH through endothelin type A receptors and by stimulating their proliferation through endothelin type B (ETB) receptors. In this study, we found that FNC-B4 cells are able to migrate in response to ET-1 through the involvement of ETB receptors. Combined immunohistochemical and biochemical analyses showed that ET-1 triggered actin cytoskeletal remodeling and a dose-dependent increase in migration**

**(up to 6-fold). Whereas the ETB receptor antagonist (B-BQ788) blunted the ET-1-induced effects, the ETA receptor antagonist (A-BQ123) did not. Moreover, we observed that FNC-B4 cells were independently and selectively stimulated by ET-1 and GnRH. We suggest that ET-1, through ETB receptor activation, may be required to maintain an adequate proliferative stem cell pool in the developing olfactory epithelium and the subsequent commitment to GnRH neuronal migratory pattern. The coordinate interaction between ET receptors and GnRH receptor participates in the fully expressed GnRH-secreting neuron phenotype. (*Endocrinology* 146: 4321–4330, 2005)**

**H**OW CELLS INITIATE, maintain, and stop their migration remains a fascinating problem in many developmental systems. Although the GnRH-secreting neurons are located postnatally within the forebrain, during embryogenesis, they arise from the olfactory placode and then migrate into the hypothalamus (1, 2). Proper spatio-temporal expression of transcription factors plays a crucial role in these processes, both in guiding GnRH-secreting neurons during their migration and in orchestrating their subsequent differentiation (3). Although the endothelin (ET) family was initially characterized as potent vasoactive peptides, a variety of other biological functions were subsequently discovered, such as stimulation of hormone release and regulation of central nervous system activity (4–7). In particular, ET immunoreactivity (8) and ET receptors (9) are present in median eminence and arcuate nucleus, in which GnRH neurons are mostly concentrated. Interestingly, ET peptides stimulate GnRH release from hypothalamic ex-

plants (10), fetal rat hypothalamic neurons (11), and fetal human olfactory cells (12).

Recent gene-inactivation studies of the components of the ET pathway have revealed some other unexpected roles of these peptides, especially during mammalian development. Mice deficient in endothelin-1 (ET-1), endothelin type A (ETA) receptor, and endothelin-converting enzyme-1 have defects in the development of subsets of cephalic and cardiac neural crest derivatives, including branchial arch-derived craniofacial tissues, and great vessel and cardiac outflow structures (13–16). Mice deficient in endothelin-3 (ET-3) or endothelin type B (ETB) receptor show spotted coat color and aganglionic megacolon due to defects in the development of neural crest-derived melanocytes and enteric neurons, respectively (17, 18). In humans, multigenic Hirschsprung's disease, or congenital aganglionosis of the distal gut, is caused by a failure of the neural crest cells to form ganglia in the distal part of the gut. This disease is characterized by pigmentation defects, deafness, and megacolon (19–21). New insights into the pathogenesis and the molecular basis of this abnormality in humans have been gained from the identification of certain critical genes, such as ET-3 and the ETB receptor in mice. These genes play a role in the development of the peripheral nervous system and in that of the connective tissue in the face, neck, and heart (22, 23). Recent research has demonstrated that genetic interactions between mutations in receptor for glial-derived neurotrophic factors (RET, receptor protein tyrosine kinase) and the ETB receptor is one of the underlying mechanisms for this complex dis-

First Published Online June 30, 2005

Abbreviations: AOD, Assay-on-demand;  $[Ca^{2+}]_i$ , intracellular calcium; ET-1, endothelin-1; ET-3, endothelin-3; ETA, endothelin type A; ETB, endothelin type B; F-actin, filamentous actin; hfPSMC, human penile smooth muscle cells; HPF, high-power field; HUVEC, human umbilical vascular endothelial cells; ns, not significant; NSE, neuron-specific enolase; SFM, serum-free medium.

*Endocrinology* is published monthly by The Endocrine Society (<http://www.endo-society.org>), the foremost professional society serving the endocrine community.

order (24). Furthermore, the interaction between the RET and ETB receptor loci in humans and mice regulates enteric nervous system development in the distal colon. It also regulates the coordinated and balanced interaction between RET and ETB receptor signaling pathways and controls the development of the mammalian enteric nervous system throughout the intestine (25). Recently, it has been demonstrated that temporally distinct requirements for ETB receptor occur in the proliferation and migration of gut neural crest stem cells (26). In a previous research, we showed that GnRH-secreting neurons, FNC-B4 cells, produce and respond to ET-1 and that this peptide regulates GnRH-secretion or cell proliferation, depending on which subtype of the ET receptor is activated (12). Moreover, GnRH acts in an autocrine/paracrine pattern to promote migration of FNC-B4 neuroblasts (27). The aim of this study was to elucidate the role played by ET-1 in the migratory pattern of GnRH-secreting neurons. FNC-B4 cells dose dependently migrated in response to ET-1 through the involvement of ETB receptor. We also report that GnRH and ET-1 act in a biologically independent and selective manner, and their recruitment is able to elicit a functional crosstalk during migration.

## Materials and Methods

### Cell cultures

The primary human GnRH-secreting neuronal cell line, FNC-B4 cells, has been established, cloned, and propagated *in vitro* from the fetal olfactory system and cryogenically preserved. FNC-B4 cells have been phenotypically, biochemically, and functionally characterized (12, 27–31). These cells grow as a monolayer, are nontumorigenic, and have a normal human karyotype. The immortalized GnRH-expressing neuronal cell line, GN11 cells, was used in some experiments (generously provided by S. Radovick, University of Chicago, Chicago, IL). GN11 neuronal cells have been isolated from olfactory bulb tumors of migration-arrested GnRH neurons (32). The human neuroblastoma SH-SY5Y cell line, a clonal derivative from primary tumor of neural crest cells, was used in some experiments [these cells are commercially available from American Type Culture Collection (Manassas, VA) and LGC Promochem (Teddington, UK)]. This cell line has been previously established and extensively characterized both phenotypically and biochemically (33–35). The primary human GnRH-secreting neuronal cell line FNC-B4, the immortalized GnRH-expressing neuronal cell line GN11, and the SH-SY5Y cell line show different biochemical and functional neuronal features that mimic some of the biochemical and functional heterogeneity that is characteristic of the developing nervous system. These cell types were cultured at 37 C in 5% CO<sub>2</sub> atmosphere in Coon's modified F-12 medium (Irvine Scientific, Santa Ana, CA), supplemented with 4.5 g/l glucose, 10% fetal bovine serum (Eurobio, Les Ulis, France), and antibiotic/antimycotic solution (penicillin, 100 IU/ml; streptomycin, 100 µg/ml).

### Chemicals

[<sup>125</sup>I]GnRH (2200 Ci/mmol) was obtained from PerkinElmer Life Science Products (Milan, Italy). [<sup>125</sup>I]ET-1 (2000 Ci/mmol) was purchased from Amersham Biosciences (Amity PG, Milan, Italy). A GnRH RIA kit was obtained from Buhlmann Laboratories (Allschwil, Switzerland). Unlabeled ET-1 and the ETA-selective antagonist A-BQ123 were obtained from NovaBiochem (Laufelfingen, Switzerland). The ETB-selective agonist IRL-1620 and antagonist B-BQ788 were purchased from Alexis (Laufelfingen, Switzerland). The polyclonal antibodies to ET-1 (RAS 6901) were purchased from Peninsula Laboratories (San Carlos, CA). Synthetic GnRH was obtained from Incstar (Stillwater, MN). GnRH agonist buserelin (D-tert-butyl-Ser6-des-Gly10-Pro9-ethylamide-GnRH) was purchased from Sigma (St. Louis, MO). GnRH antagonist cetrorelix [Ac-D-Nal (2)1, D-Phe (4Cl)2, D-Pal (3)3, D-Cit6, D-Ala10] was purchased from ASTA Medica (Frankfurt, Germany). The rabbit polyclonal anti-

bodies to the ETA and ETB receptors were provided by Assay Design (Ann Arbor, MI) and were used at 1:100 concentration; the anti-goat polyclonal neuron-specific enolase (NSE) antibody (1:100 dilution) sc-7455 was purchased from Santa Cruz Biotechnology (Santa Cruz, CA). 3,4,3',4', Tetra-aminodiphenylhydrochloride (diaminobenzidine) was obtained from BDH Chemicals (Poole, UK). Streptavidin-biotin peroxidase complex kits were obtained from Dako (Carpinteria, CA). Other reagents were obtained at the highest grade available from commercial sources or from Sigma.

### Isolation of RNA and cDNA synthesis

Total RNA was extracted from cells using RNAase mini kit from Qiagen (Valencia, CA) according to the instructions of the manufacturer. RNA concentration and quality were measured by spectrophotometric analysis at 260 and 280 nm. RNA integrity was assessed by electrophoresis in agarose gel. Total RNA (400 ng) was reverse transcribed to cDNA in a final volume of 80 µl using TaqMan Reverse Transcription kit (Applied Biosystems, Foster City, CA) at the following conditions: 10 min at 25 C, 30 min at 48 C, and 5 min at 95 C.

### Real-time quantitative RT-PCR

The mRNA quantitative analysis was performed according to the fluorescent TaqMan methodology, as published previously (36). PCR primers and probe for mRNA quantitation of ET-1 receptors (ETA and ETB) were purchased as an assay-on-demand (AOD) gene expression product from Applied Biosystems. The glyceraldehyde-3-phosphate dehydrogenase gene was chosen as the reference gene, and the corresponding AOD product was provided by Applied Biosystems. The PCR mixture (25 µl final volume) consisted of 1× final concentration of AOD mix, 1× final concentration of Universal PCR Master mix (Applied Biosystems), and 25 ng cDNA. Amplification and detection were performed with an ABI Prism 7700 Sequence Detection System (version 1.7) (Applied Biosystems) with the following thermal cycler conditions: 2 min at 50 C, 10 min at 95 C, and 40 cycles at 95 C for 30 sec and 60 C for 1 min. Each measurement was performed in duplicate. mRNA quantitation was based on the comparative C<sub>T</sub> method, according to the instructions of the manufacturer, in which C<sub>T</sub> represents the cycle number at which the fluorescent signal, associated with an exponential increase in PCR products, crossed a given threshold. The maximum change in C<sub>T</sub> values of the sample ( $\Delta C_{T \text{ sample}}$ ) was determined by subtracting the average of duplicate C<sub>T</sub> values of the reference gene from the average of the duplicate C<sub>T</sub> values of the target gene. Human umbilical vascular endothelial cells (HUVEC) (37), classically considered positive targets for ETB ligands, together with the SH-SY5Y cell line, were used as controls.

### Measurement of intracellular calcium concentration

Digital video imaging of the intracellular-free calcium concentration ([Ca<sup>2+</sup>]<sub>i</sub>) in individual human FNC-B4 cells was performed as described previously (27). Human neurons were grown to subconfluence in complete culture medium on round glass coverslips (25-mm diameter, 0.2-mm thick) for 72 h and then incubated for 48 h in serum-free medium (SFM) at 37 C. Cells were then loaded with 10 µmol/l fura 2-AM and 15% Pluronic F-127 for 30 min at 22 C. [Ca<sup>2+</sup>]<sub>i</sub> was measured in fura 2-loaded cells in HEPES-NaHCO<sub>3</sub> buffer containing the following (in mmol/l): 140 NaCl, 3 KCl, 0.5 NaH<sub>2</sub>PO<sub>4</sub>, 12 NaHCO<sub>3</sub>, 1.2 MgCl<sub>2</sub>, 1.0 CaCl<sub>2</sub>, 10 HEPES, and 10 glucose (pH 7.4). Ratio images (340/380 nm) were collected every 3 sec, and calibration curves were obtained for each cell preparation. ET-1, ETA, and ETB receptor antagonists (A-BQ123 and B-BQ788), GnRH and/or its analog (buserelin), and GnRH antagonist (cetrorelix) (from 0.1 µM to 1 nM) were directly added to the perfusion chamber immediately after recording the [Ca<sup>2+</sup>]<sub>i</sub> basal value. In parallel experiments, cells were preincubated with 0.1 µM ETB receptor antagonist for 10 min before addition of ET-1. These experiments were done in triplicate.

### Immunocytochemical procedures and confocal laser microscopy

FNC-B4 cells were cultured on glass coverslips in SFM for 18 h and then left untreated or incubated with ET-1. Cells were then fixed with

3.7% paraformaldehyde (pH 7.4) for 10 min and then permeabilized for 10 min with PBS ( $\text{Ca}^{2+}$ / $\text{Mg}^{2+}$ -free), containing 0.1% Triton X-100. Immunostaining was performed as described previously (12, 23), using polyclonal antibodies to ETA and ETB receptor (1:50), followed by streptavidin-biotin peroxidase complex (LSAB kit; Dako). The specificity of the anti-ETA and ETB receptor antibodies was controlled by preabsorption of the primary antibodies with a membrane preparation from human fetal penile smooth muscle cells (hfPSMC), particularly enriched in the respective receptors, as detected by binding experiments (38), according to a previously described method (39). Briefly, ETA and ETB receptor antibodies (working dilution) were incubated with 1 mg/ml hfPSMC membranes in 50 mM Tris HCl buffer, or with buffer only, overnight at 4 C. After an additional 60-min incubation with 4% polyethylene glycol, the unbound antibodies were separated by rapid centrifugation and used for immunohistochemistry. Filamentous actin (F-actin) was stained with rhodamine phalloidin (1:50; Molecular Probes, Eugene, OR) in the permeabilization solution for 45 min at room temperature. Cells were viewed with a laser scanner confocal microscope (MRC 600; Bio-Rad, Hercules, CA), equipped with a Nikon (Tokyo, Japan) diaphot inverted microscope or with a Nikon Microphot-FX microscope. The percentages shown in Figure 3 concerning various morphologies of actin-based cell deformations (i.e. percentage of cells showing at least two of the following morphological features: actin patches, filopodia, lamellipodia, and membrane ruffles) were obtained

by counting the number of activated cells over the total number of stained cells from three different experiments (at least three slides for each experiment and five fields from each slide).

### GnRH and ET-1 RIA

Immunoreactive GnRH was extracted from conditioned media of FNC-B4 cells with chilled absolute ethanol ( $-20\text{ C}$ ), evaporated to dryness, and subjected to RIA using a commercial kit (Buhlmann Laboratories), as described previously (31). Immunoreactive ET-1 was extracted from conditioned media of FNC-B4 cells using Sep-Pak C18 cartridges (Millipore, Milford, MA), as described previously (12). The specific RIA for ET-1 was performed in 0.1 M PBS [0.1% Triton X-100, 0.1% BSA, and 0.01%  $\text{NaN}_3$  (pH 7.4)] by a two-step incubation procedure. Samples and standards (0.1 ml) were incubated at 4 C overnight with the respective antiserum (ET-1: RAS6901, 1:20,000, 0.1 ml) and further incubated with the respective tracer (0.1 ml, 10 pM) at 4 C overnight. Bound/free separation was performed by a second antibody/polyethylene glycol procedure.

### SDS-PAGE, Western blot analysis, and immunoblotting

FNC-B4 cells, grown to confluence, were scraped into PBS ( $\text{Ca}^{2+}$ / $\text{Mg}^{2+}$ -free), centrifuged, and resuspended in lysis buffer [20 mM Tris-HCl, 150 mM NaCl, 0.25% Nonidet P-40, 1 mM  $\text{Na}_3\text{VO}_4$ , 1 mM phenyl-

A

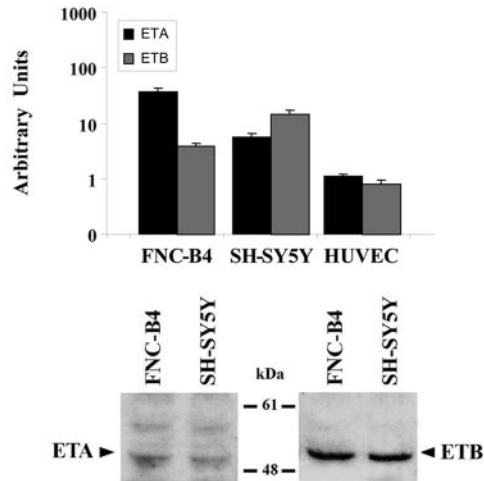


FIG. 1. A, Quantitative gene expression of ET-1 receptors in FNC-B4 cells and SH-SY5Y. The *top* shows the quantitative detection of mRNA (RT-PCR) for ETA and ETB receptors in FNC-B4 and SH-SY5Y neural cells. Expression of the same genes in HUVEC was also shown for comparison. ETB transcripts were definitively higher in GnRH-secreting neurons and neuroblastoma cells than in endothelial cells, used as positive control. Data (mean  $\pm$  SD;  $n = 3$ ) are expressed in arbitrary units, calculated according to the comparative  $C_T$  method and normalized to the glyceraldehyde-3-phosphate dehydrogenase, chosen as reference gene. The *bottom* shows the expression of ETA and ETB proteins in the same neuronal cells, as determined by Western blot analysis. Specific bands, of the expected sizes, were detected using rabbit polyclonal antibodies against ETA (*left*) and ETB (*right*) receptors. B, Immunohistochemistry for ET-1 receptors in FNC-B4 neurons. The intracellular localization of ETA (panel a) and ETB (panel b) receptors in FNC-B4 was revealed by the same antibodies as in A (*bottom*). Note the positivity for ETA and ETB receptors in the perinuclear cytoplasmic compartment, with a fading localization within the tiny cytoplasmic protrusions (see *arrows*). Positive staining for both ETA (panel c) and ETB (panel d) receptors disappeared after preabsorbing the two antibodies with a membrane preparation from hfPSMC, enriched in the respective receptors. Scale bar, 0.3  $\mu\text{m}$ .

B

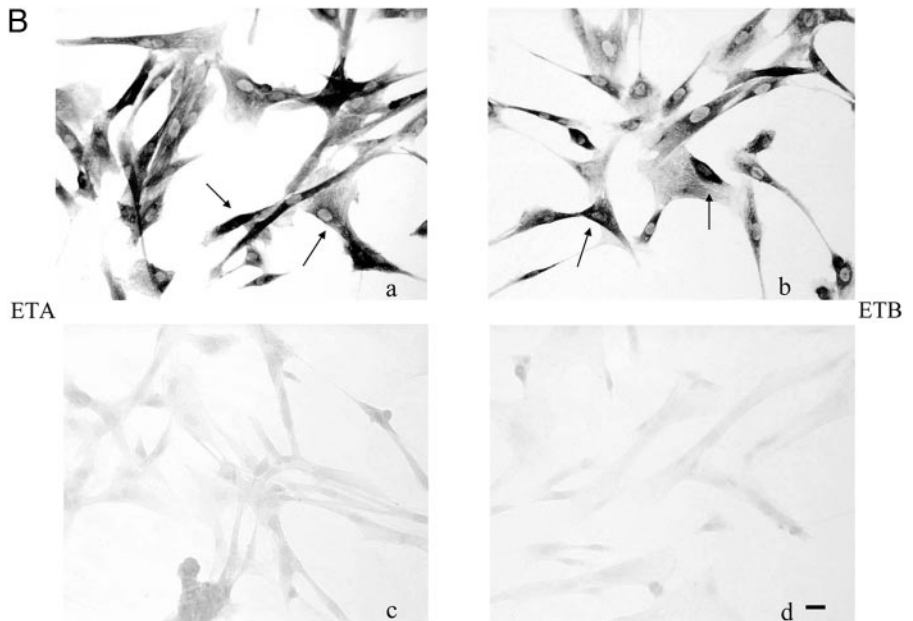
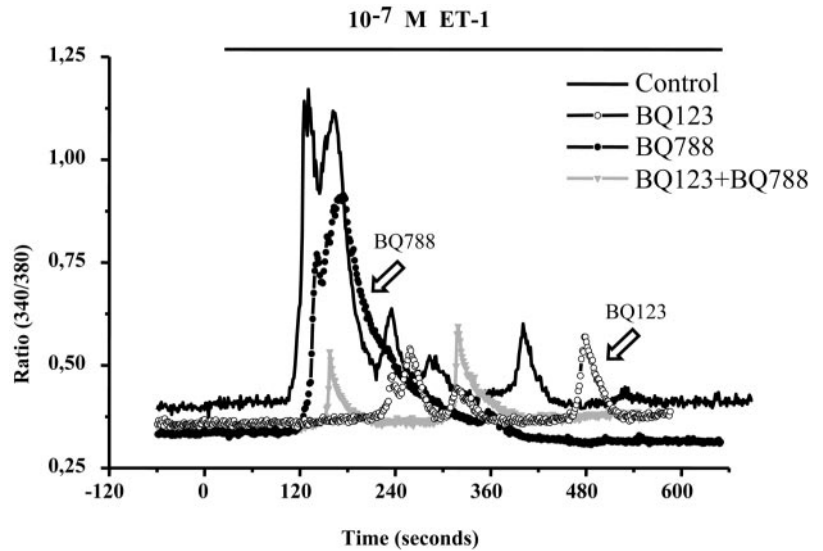


FIG. 2. Measurement of intracellular calcium concentration. Digital video imaging of  $[Ca^{2+}]_i$  in individual human FNC-B4 cells. ET-1, BQ123 and BQ788, GnRH or busserelin, and cetrorelix were added directly to the perfusion chamber immediately after recording the  $[Ca^{2+}]_i$  basal value. In parallel experiments, cells were preincubated with 0.1  $\mu M$  ETB receptor antagonist for 10 min before the addition of ET-1 (black trace). BQ123 was able to almost blunt (70  $\pm$  2%)  $[Ca^{2+}]_i$  transients (white circles), whereas BQ788 abolished only 30  $\pm$  3% of cases of ET-1-induced  $[Ca^{2+}]_i$  increases (black circles). Contemporary exposure to both antagonists blunted the effects of ET-1 (gray triangles).



methylsulfonylfluoride, 1 mM EGTA (pH 7.4)]. Protein concentration was measured using a Coomassie Bio-Rad protein assay kit. Aliquots containing 30  $\mu g$  of proteins were diluted in 2 $\times$  reducing Laemmli's sample buffer [62.5 mM Tris (pH 6.8), 10% glycerol, 20% SDS, 2.5% pyronin, and 100 mM dithiothreitol] and loaded onto 10% SDS-PAGE. After SDS-PAGE, proteins were transferred to nitrocellulose membranes (Immobilon-P transfer membranes, polyvinylidene difluoride; Millipore). Membranes were blocked overnight at 4 C in 5% BSA-TTBS buffer (0.1% Tween 20, 20 mM Tris-HCl, and 150 mM NaCl), washed in TTBS, and incubated for 2 h with anti-actin primary antibody (1:1000 dilution), followed by peroxidase-conjugated secondary IgG (1:3000). Finally, the reacted proteins were revealed by enhanced chemiluminescence system (ECL; Roche Diagnostics, Basel, Switzerland). For reprobing with different antibodies, the nitrocellulose membranes were washed for 30 min at 50 C in stripping buffer [10 mM Tris (pH 6.8), 2% SDS, 100 mM b-mercaptoethanol] and reprobed with anti-glyceraldehyde 3-phosphate dehydrogenase antibody (1:1000 dilution; sc-7455; Santa Cruz Biotechnology).

#### Chemotactic assay

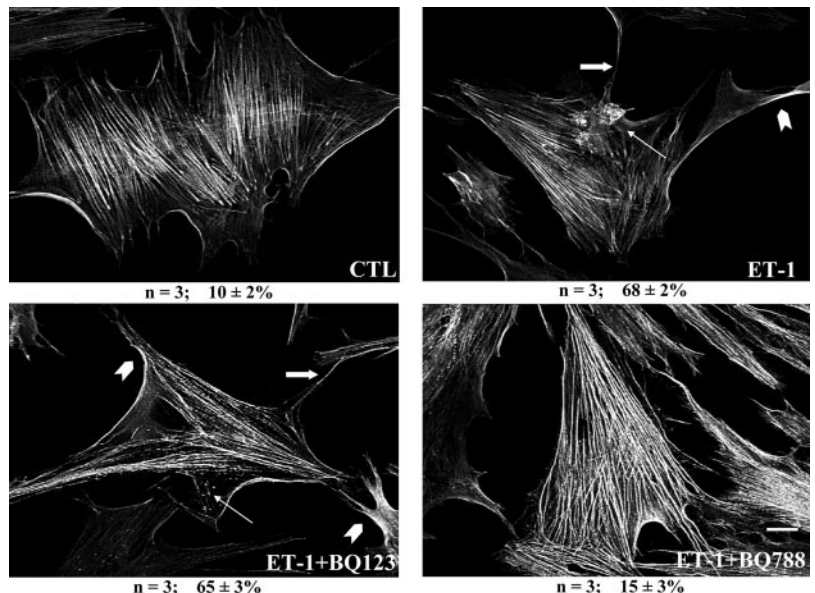
Cell migration was performed as described previously (27). Briefly, modified Boyden chambers (Nuclepore, Pleasanton, CA), each equipped with a 13-mm diameter and a 5- or 8- $\mu m$  porosity polyvinylpyrrolidone-

free polycarbonate filter were used. The filters were coated with 20  $\mu g/ml$  human type I collagen or 10  $\mu g/ml$  fibronectin (Collaborative Biomedical Products, Bedford, MA) for 30 min at 37 C. Confluent FNC-B4 cells, GN11 cells, and SH-SY5Y cells were incubated in SFM for 24 h (control conditions). After mild trypsinization with 0.05% trypsin-EDTA, in 210- $\mu l$  aliquots, each of which corresponding to  $4 \times 10^4$  cells/Boyden chamber, the cells were added to the top wells and incubated at 37 C in 5% CO<sub>2</sub> for 6 h. Increasing concentrations of ET-1, or IRL-1620, in the presence or absence of ETA and/or ETB receptor antagonists (A-BQ123 or B-BQ788; 10<sup>-7</sup> M concentration), and GnRH or busserelin, in the presence or absence of cetrorelix (10<sup>-7</sup> M concentration), were added to the bottom chambers. Both ET-1 and GnRH were incubated in the presence of cetrorelix or A-BQ123/B-BQ788, respectively. After incubation, the migrated cells were fixed in 96% methanol and stained with Diff Quick solution (Biomap, Milan, Italy) or Harris' hematoxylin solution. Chemotaxis was quantitated by randomly counting six chosen fields per filter, and results were expressed as the number of cells per high-power field (HPF).

#### Statistical analysis

Data are expressed as the mean  $\pm$  SD. An one-way ANOVA followed by *post hoc* test (Bonferroni's correction for multiple comparisons) was

FIG. 3. Effects of ETB receptor activation in FNC-B4 neurons on F-actin. FNC-B4 cells were cultured on glass coverslips in SFM for 24 h and then left untreated (CTL) or incubated for 18 h with ET-1 (10<sup>-7</sup> M). F-actin, after fixation, was visualized with rhodamine phalloidin (1:50) in the permeabilization solution for 45 min at room temperature. Cells were viewed with a laser scanner confocal microscope. A typical pattern of expression of F-actin in unstimulated FNC-B4 cells is shown (CTL). ET-1 (100 nM) exerted striking activation of cell morphology, together with actin stress fiber network, toward a spindle-like shape, with actin-based cell deformation and the presence of actin patches (thin arrow), together with the appearance of lamellipodia (arrowhead) and filopodia (thick arrow) on the edge of cell membranes (ET-1). Simultaneous incubation with ET-1 (100 nM) and BQ123 (100 nM) induced similar actin-based cytoskeletal modifications than ET-1 alone (ET-1+BQ123) (see arrows); vice versa, coincubation of ET-1 (100 nM) and BQ788 (100 nM) did not induce morphological changes different from controls (ET-1+BQ788). Scale bar, 0.15  $\mu m$ .



performed. The level of  $P < 0.05$  was accepted as statistically significant. Comparisons of percentages were analyzed statistically after conversion through arc-sine transformation from the binomial to the normal distribution. The computer program ALLFIT was used for the analysis of the sigmoidal dose-response curves (40).

## Results

### ETB receptor expression in human FNC-B4 cells

Figure 1A (*top*) shows ETA and ETB mRNA expression (quantitative RT-PCR) in neuronal compared with endothelial cells, taken as positive controls. Both GnRH-secreting neurons and neuroblastoma cells express, respectively, a 4- and 15-fold higher concentration of ETB transcripts than HUVEC, classically considered positive targets for ETB ligands (37). Western blot analysis with polyclonal anti-ETA and anti-ETB antibodies (Fig. 1A, *bottom*) shows specific bands for both receptors, at the expected molecular weight, in both FNC-B4 or SH-SY5Y cells. The intracellular immunodistribution of ETA and ETB in FNC-B4 cells is shown in Fig. 1B. Note the positivity for both receptors in the perinuclear cytoplasmic compartment, with a fading localization within the tiny cytoplasmic protrusions (Fig. 1B).

### Intracellular signaling activated by ET-1 in FNC-B4 cells

A typical experiment on ET-1-induced intracellular calcium mobilization in fura 2-loaded FNC-B4 cells is shown in Figure 2. ET-1 ( $10^{-7}$  M) induced in control cells a transient and sustained activation of calcium waves. This stimulation was partially blunted by the ETB antagonist B-BQ788, although it was substantially inhibited by the ETA antagonist A-BQ123. Quantitative analysis of multiple results (data not shown) indicated that A-BQ123 inhibits  $70 \pm 2\%$  and B-BQ788 inhibits  $30 \pm 3\%$  of the ET-1-induced calcium mobilization. Only the simultaneous presence of both antagonists almost abolished ET-1-stimulated calcium transients (Fig. 2). These results suggest that both receptors are involved in mobilizing intracellular calcium in FNC-B4 cells.

### Biological effects of ETB receptor activation in FNC-B4 neurons

Unstimulated FNC-B4 cells showed an intense actin stress fiber network, as detected by F-actin conjugated with rhodamine phalloidin (Fig. 3, *CTL*). In this assay, a small fraction ( $10 \pm 2\%$ ;  $n = 3$ ) of unstimulated cells displayed actin cytoskeletal remodeling. After 18 h of exposure to ET-1 ( $10^{-7}$  M) (Fig. 3, *ET-1*), we noticed a significant increase ( $68 \pm 2\%$ ;  $n = 3$ ;  $P < 0.0005$ ; ET-1 *vs.* control) in various actin-based cell deformations, *i.e.* actin patches (*thin arrow*), filopodia (*thick arrow*), lamellipodia (*arrowhead*), and membrane ruffles. In addition, we documented an ET-1-induced development of broad lamellae, prominent lamellipodia, numerous membrane ruffles, and microspikes, compatible with a motile phenotype. A-BQ123 ( $10^{-7}$  M) was ineffective in antagonizing ET-1 effects ( $65 \pm 3\%$ ;  $n = 3$ ;  $P < 0.005$ ) (Fig. 3, *ET-1+BQ123*), whereas B-BQ788 ( $10^{-7}$  M) was able to elicit ET-1-induced phenotype modifications [ $15 \pm 3\%$ ;  $n = 3$ ;  $P$  value was not significant (ns)] (Fig. 3, *ET-1+BQ788*). These ET-1-induced cytoskeletal rearrangements were further confirmed by Western blot analysis using actin antiserum recognizing

actin protein at the expected molecular weight (Fig. 4A). ET-1 induced a significant increase ( $P < 0.023$ ) in actin expression, not reverted ( $P < 0.05$ ) by A-BQ123 but reverted by B-BQ788 ( $P$  value was ns) (Fig. 4B). To assess equal protein loading, nitrocellulose membranes were stripped and reprobbed with anti-NSE (we thus observed no significant modifications either after ET-1 exposure or inhibitors' stimulation in the presence of ET-1) (Fig. 4C). Because ET-1 induced a motile phenotype in FNC-B4 cells, we studied whether or not ET-1 induced cell migration by using the chemotactic Boyden chamber technique (cell migration toward regions at higher concentration of chemotactic factors). FNC-B4 neuronal cells responded in a migratory manner to ET-1 (Fig. 5A). In particular, FNC-B4 responded to SFM with a time-dependent increase in spontaneous random migration ( $7 \pm 1.4$  cells per HPF after 6 h of incubation;  $n = 30$ ). ET-1 stimulated a 4- to 6-fold increase in this migratory pattern in the FNC-B4 cells in a dose-dependent manner (from  $10^{-9}$  to  $10^{-7}$  M) ( $n = 12$ ;  $*$ ,  $P < 0.0005$  *vs.* SFM). Whereas the ETA receptor antagonist A-BQ123 was ineffective to completely counteract ET-1-in-

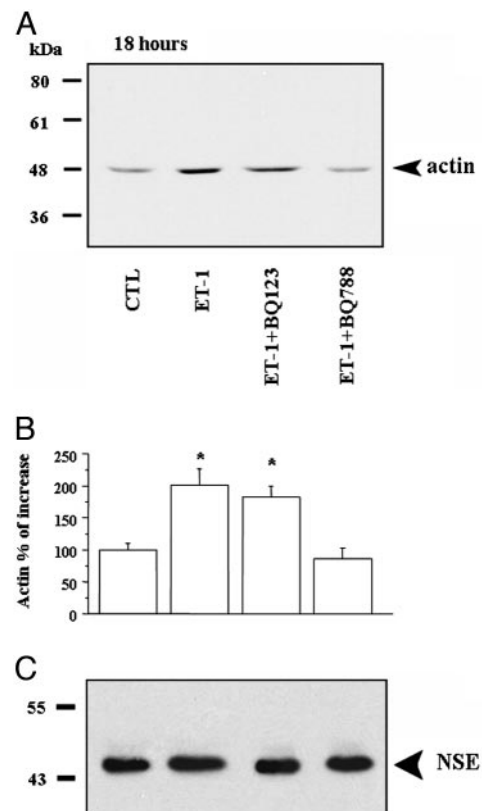


FIG. 4. Effects of ETB receptor activation on actin expression in FNC-B4 neurons. FNC-B4 cells were cultured in SFM for 24 h, incubated for 18 h with ET-1 ( $10^{-7}$  M), and then subjected to Western blot analysis of actin (A). A single protein band, migrating at the expected molecular weight, is indicated by the *arrowhead*. ET-1 stimulated actin expression ( $*$ ,  $P < 0.05$  *vs.* control). This enhanced expression was reverted by BQ788 but not by BQ123 ( $*$ ,  $P < 0.05$  *vs.* control). Quantification of actin increase is reported in B (percentage of increase in actin expression over the control value, taken as 100%). Experiments were done in triplicate.  $*$ ,  $P = 0.05$ . Nitrocellulose membranes were stripped and reprobbed with anti-NSE to assess equal protein loading (C). No modification was observed in NSE expression among lanes (data not shown). CTL, Control.

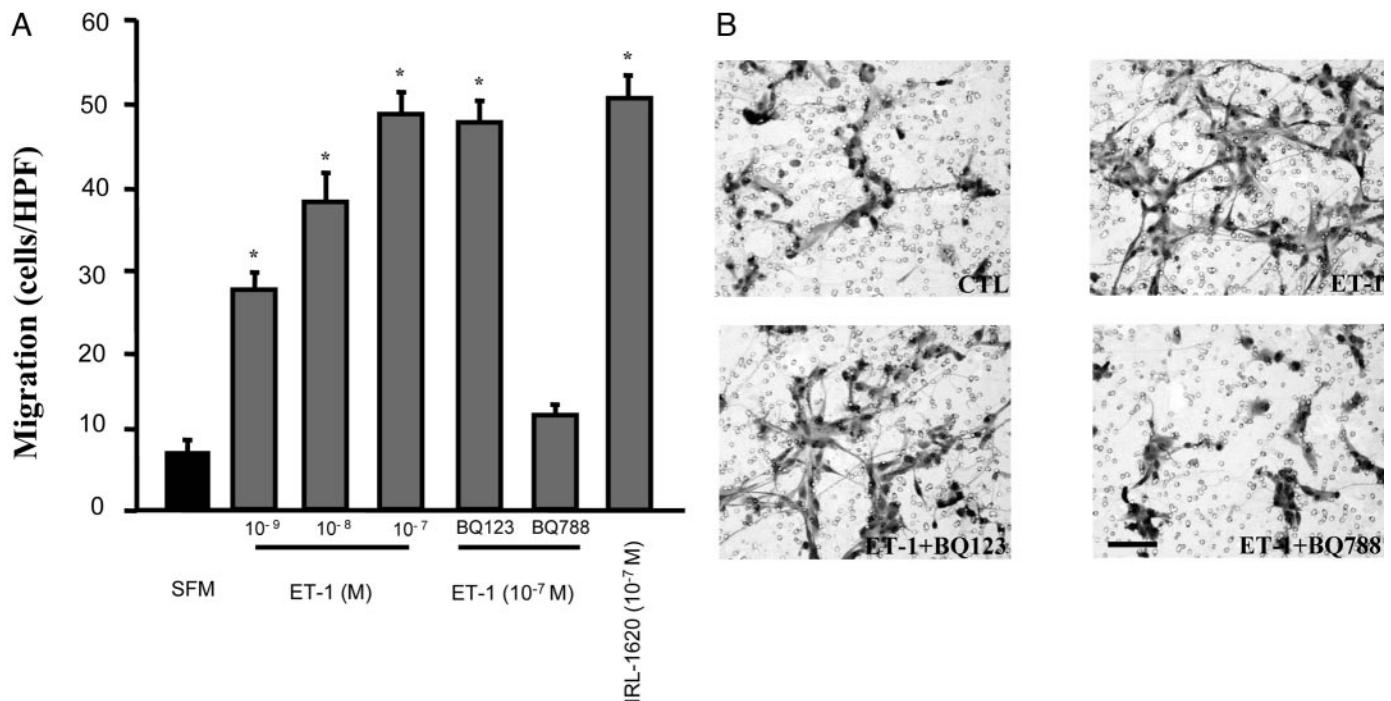


FIG. 5. Biological effects of ETB receptor activation in FNC-B4 neurons. A, Cell migration of FNC-B4 cells toward ET-1 was performed according to *Materials and Methods*. Increasing concentrations of ET-1, with BQ123 or BQ788 ( $10^{-7}$  M), were added to the bottom chambers. Effect of IRL-1620 is also shown. FNC-B4 cells responded to SFM conditions, showing spontaneous random migration [ $7 \pm 1.4$  cells per HPF after 6 h of incubation;  $n = 30$ ]. ET-1 induced a 4- to 6-fold increase in migratory pattern in FNC-B4 cells, in a dose-dependent manner (from  $10^{-9}$  to  $10^{-7}$  M; \*,  $P < 0.0005$  vs. control conditions, SFM). IRL-1620 ( $10^{-7}$  M) induced a similar increase to an equimolar concentration of ET-1 (\*,  $P < 0.0005$  vs. control). BQ788 counteracted ET-1 effects, whereas BQ123 did not reduce ET-1-induced migration (\*,  $P < 0.0005$ ;  $n = 12$ ). B, A representative pattern of migrating cells on Boyden chamber filters, under different experimental conditions, is shown. Scale bar,  $0.03 \mu\text{m}$ .

duced migratory pattern ( $n = 12$ ; \*,  $P < 0.0005$  vs. SFM), the ETB receptor antagonist B-BQ788 was able to blunt this effect ( $P$  value was ns). The data suggest the main involvement of ETB receptor in the migration of FNC-B4. This was further confirmed by the incubation with an ETB receptor-selective agonist (IRL-1620,  $10^{-7}$  M) ( $n = 12$ ; \*,  $P < 0.0005$  vs. SFM). A representative pattern of migrating cells on the Boyden chamber filters is shown in Figure 5B. In particular, ET-1 induced a migratory pattern characterized by a huge recruitment of cell populations that maintained close connections with one another, which was blunted only by B-BQ788. We also tested the migratory activity of ET-1 in two other cell lines, GN11 and SH-SY-5Y. The immortalized GN11 cells, intrinsically motile like GnRH cells, provided an excellent cellular model of migrating GnRH neurons that are arrested during their transit to the brain. The human neuroblastoma SH-SY-5Y cell line, a clonal derivative from primary tumors of neural crest cells, represented a valid model of the invasive behavior of neural crest cells. Even in these cell lines ET-1 ( $10^{-7}$  and  $10^{-8}$  M) induced a strictly ETB-dependent migratory pattern. In fact, in both GN11 ( $n = 4$ ) and SH-SY5Y ( $n = 3$ ) cells, ET-1 induced a significant ( $P < 0.0005$ ) increase in cell migration, which was completely abolished by B-BQ788 but not by A-BQ123 (Fig. 6, A and B).

#### Crosstalk of ET-1 and GnRH peptides in FNC-B4 neurons

The aforementioned results, taken together, strongly suggest that ET-1 induced migration in neural cells and, in par-

ticular, in GnRH-producing cells, through ETB receptors. Previous studies have demonstrated that FNC-B4 cells produce and respond to ET-1; this peptide not only positively regulates GnRH secretion (acting through the ETA receptors) but also stimulates proliferation (acting through ETB receptors) (12). GnRH induced in the same cells GnRH release and a clear migratory pattern (27). Now we observed GnRH-induced ET-1 production that is able to elicit FNC-B4 cell migration. The aim of this study was also to investigate whether migration and release due to GnRH were, at least partially, mediated by a GnRH-induced activation of ET-1 signaling. We found that, in FNC-B4 cells, increasing concentrations ( $10^{-12}$  to  $10^{-6}$  M) of buserelin, a GnRH agonist, induced a 9-fold increase in ET-1 release ( $EC_{50}$  of  $0.95 \pm 0.17$  nM;  $n = 3$ ) (Fig. 7). To test whether an ET-1-driven autocrine loop was involved in GnRH-induced GnRH secretion, we performed GnRH release experiments in the presence of selective receptor antagonists. As reported previously (12, 27), both buserelin and ET-1 ( $10^{-7}$  M) stimulated GnRH secretion (Fig. 8), which was only abolished by their cognate antagonists. In fact, neither the ET-1 antagonists A-BQ123/B-BQ788 nor cetrorelix affected GnRH secretion induced by buserelin and ET-1, respectively. Interestingly, only A-BQ123 blunted the stimulatory effect of ET-1, thus confirming the involvement of ETA receptors in GnRH secretion ( $n = 4$ ; \*,  $P < 0.0005$  vs. control value = 100%) (12). The specific GnRH antagonist cetrorelix ( $10^{-7}$  M) blunted GnRH-induced release in the presence of buserelin, although it did not modify

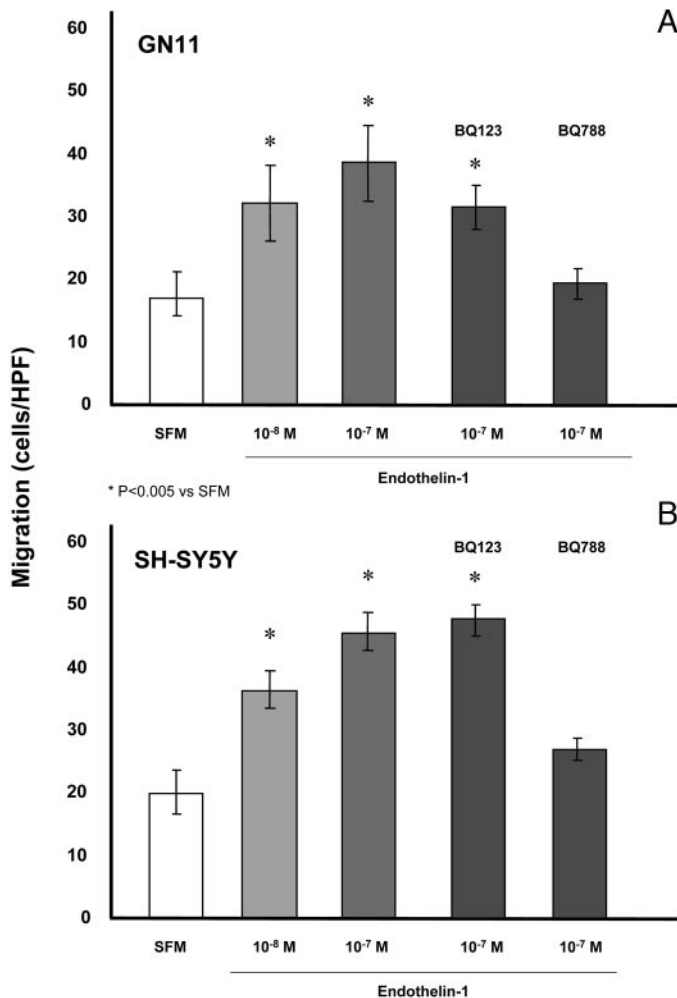


FIG. 6. Migration of GN11 or SH-SY5Y cells toward ET-1. Effect of ET-1 ( $10^{-8}$  and  $10^{-7}$  M), with or without BQ123 or BQ788 ( $10^{-7}$  M), on cell migration of GN11 (A) or SH-SY5Y (B), performed according to *Materials and Methods*. ET-1 at all the concentration tested induced in both GN11 cells and in the human neuroblastoma SH-SY5Y cells a significant (\*,  $P < 0.0005$ ) increase in migratory pattern. ET-1 ( $10^{-7}$  M)-induced cell migration was completely counteracted by an equimolar concentration of BQ788 but not of BQ123 (\*,  $P < 0.0005$  vs. control).

GnRH release in the presence of ET-1 ( $n = 4$ ; \*,  $P < 0.0005$  vs. control value = 100%). Similar results were obtained through cell migration. As shown in Fig 9, we observed a higher degree of migratory potency of the ET-1 peptide with respect to the GnRH peptide (a 4- to 6-fold increase with respect to a 3- to 4-fold increase;  $n = 6$ ; \*,  $P < 0.0005$  vs. control conditions). Similar results were observed after stimulation of cells with the GnRH analog busserelin (data not shown). Furthermore, we observed that the ETA receptor antagonist A-BQ123 was ineffective in the presence of either ET-1 ( $10^{-7}$  M) ( $n = 6$ ; \*,  $P < 0.0005$  vs. control) or GnRH (at the same concentration) ( $n = 6$ ; \*,  $P < 0.0005$  vs. control) stimulation. However, ETB receptor antagonist B-BQ788, effective in counteracting ET-1 migration ( $n = 6$ ; \*,  $P$  values were ns), did not significantly blunt the GnRH-induced migrating capacity ( $n = 6$ ; \*,  $P < 0.0005$  vs. control). Cetrorelix was able to blunt GnRH migration ( $n = 6$ ; \*,  $P$  value was ns), although it was

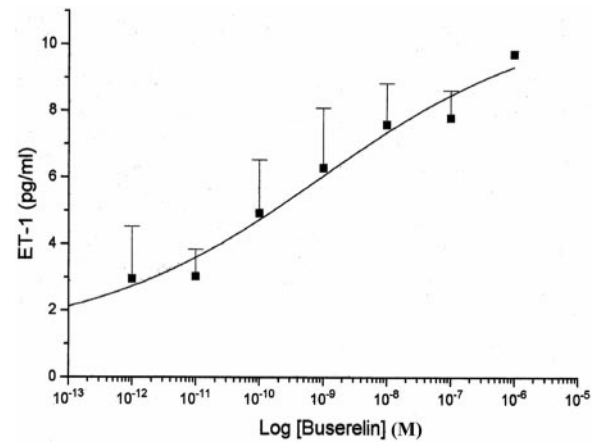


FIG. 7. Crosstalk of ET-1 and GnRH peptides in FNC-B4 neurons. Effects of GnRH on ET-1 production in FNC-B4 neurons. RIA of ET-1 in conditioned media from FNC-B4 cells. In the presence of increasing concentrations of busserelin (from  $10^{-12}$  to  $10^{-6}$  M), a dose-dependent 9-fold increase in ET-1 secretion ( $EC_{50}$  of  $0.95 \pm 0.17$  nM;  $n = 3$ ) was observed.

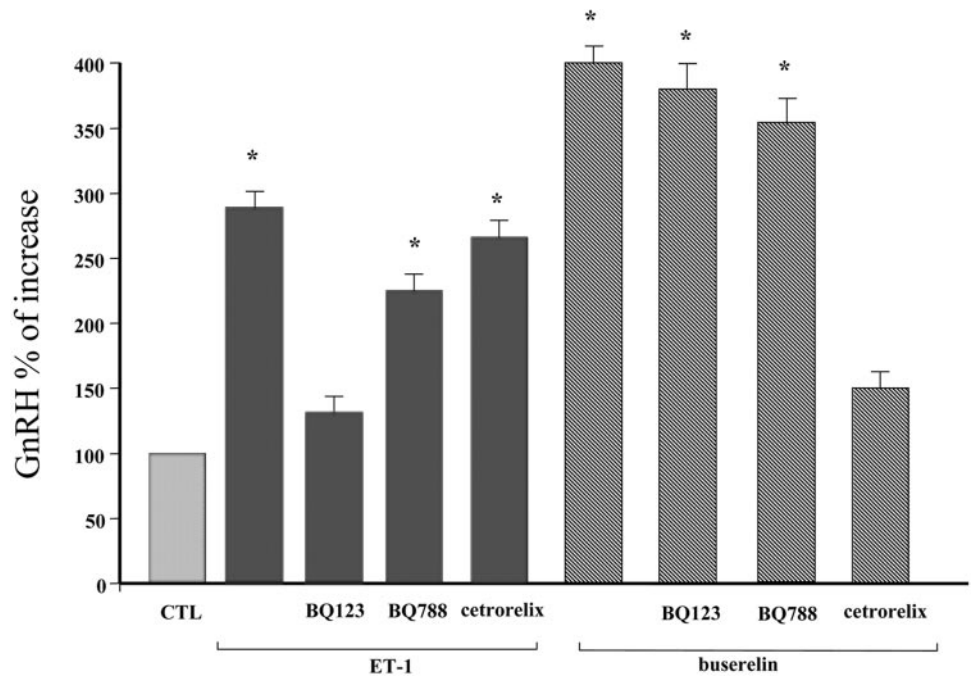
ineffective in blunting ET-1-induced migration ( $n = 6$ ; \*,  $P < 0.0005$  vs. control) (Fig. 9).

## Discussion

This study is the first to document that human olfactory GnRH-secreting neuroblasts, FNC-B4 cells, are able to migrate in response to ET-1. This ability to migrate was observed also in the immortalized mouse GnRH-expressing neuronal cell line GN11. A striking feature of this report is that ET-1 migration was elicited by selective ETB receptor recruitment and was completely independent of the previously reported ETA-induced GnRH secretion (12). Primary human GnRH-secreting neuroblasts FNC-B4, established from fetal olfactory epithelium, and immortalized GnRH-expressing neuronal cell line GN11, isolated from an olfactory tumor of migration-arrested GnRH neurons, retain properties found *in vivo* in either the early or the later stages of GnRH neuronal navigation (27, 29, 31, 41, 42). Thus, these cell lines represent excellent models to study prenatal GnRH neurons. The results herein presented show that ET-1 recruitment is due to ETB receptor activation. By using ETB receptor antagonist B-BQ788, a significant inhibition of ET-1-induced migration was observed. FNC-B4 cells present two different binding receptors, *i.e.* the ETA and ETB receptors. These two classes of molecules are involved in different biological responses. ETA receptor recruitment induced GnRH secretion, whereas ETB receptor stimulated DNA synthesis (12). In this report, we show that ET-1, through ETB receptor recruitment, was able to trigger a striking morphological activation of cells toward a clear migratory pattern and intracellular calcium increase. ET-1 induced modifications in cell shape and development of cytoplasmic protrusions and lamellipodia extensions, associated with actin protein expression. This recruitment led to the formation of a huge intercellular network, which probably constituted the morphological basis of cell activation and the consequent induction of multiple intercellular crosstalks (3).

Previous researches has demonstrated that FNC-B4 cells

FIG. 8. Effects of ET-1 and GnRH agonists and antagonists on GnRH release from FNC-B4 cells. ET-1 ( $10^{-7}$  M) and buserelin ( $10^{-7}$  M) induced 3-fold and 4-fold increase, respectively, in GnRH secretion (both \*,  $P < 0.0005$  vs. control). ET-1 stimulation on GnRH release was unaffected by BQ788 ( $10^{-7}$  M; \*,  $P < 0.0005$  vs. control) and cetrorelix ( $10^{-7}$  M; \*,  $P < 0.0005$  vs. control) but almost completely blunted by BQ123 ( $10^{-7}$  M). Buserelin stimulation was unaffected by both ET-1 antagonists (both \*,  $P < 0.0005$  vs. control) but completely abrogated by cetrorelix. Columns indicate the percentage of increase in GnRH secretion over the control value (100%), as measured by RIA. Experiments were done in triplicate. CTL, Control.

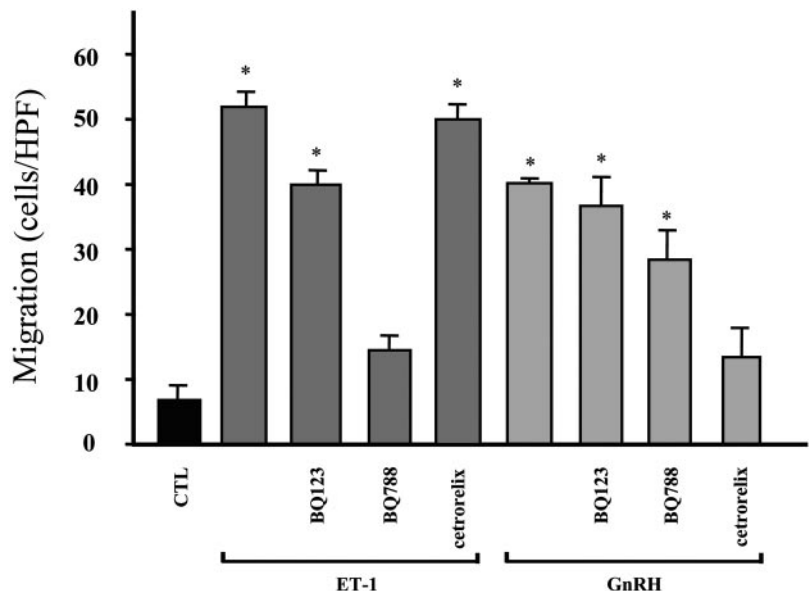


express ET-1 and respond to ET-1 through a GnRH release, which, in turn, was able to induce FNC-B4 cells to migrate (12, 27). Here, we demonstrate that GnRH stimulated ET-1 release. Because ET-1 stimulated motility and GnRH release, we investigated whether these GnRH-related effects may be, at least partially, mediated by a GnRH-induced activation of ET-1 signaling. Our findings suggest a crosstalk between these two neuropeptides. In fact, functional data, by using selective antagonists, indicate that FNC-B4 cells were independently and selectively stimulated by the two different peptides. Thus, ET-1, through ETA/ETB and GnRH receptor crosstalk, may participate in differentiation of the neuroendocrine phenotype of FNC-B4 olfactory neuroblasts.

In the olfactory epithelium, proliferation of neural precursor cells and differentiation of their progeny into olfactory

receptor neurons begin during embryogenesis and continue throughout life (43, 44). The ET-3/ETB pathway has the potential to differentiate neural crest cells to multipotent precursors (45–47). Thus, exposure of FNC-B4 neuroblasts to ET-1 may lead to different stages of differentiation of functional activation. The first one is characterized by an immature and undifferentiated stage, with a huge proliferative commitment, and the second one, more differentiated, is characterized by morphological and cytoskeletal activation, the acquisition of clear chemotactic properties, and the recruitment of both subtypes of ET and GnRH receptors. These receptors, together with functional recruitment of both GnRH and ET-1 molecules, are able to crosstalk and interact with each other (the so-called “loop activity between ET and GnRH”). We suggest that the onset of this activity loop plays

FIG. 9. Effects of ET-1 and GnRH agonists and antagonists on FNC-B4 migration. ET-1 or GnRH ( $10^{-7}$  M), with or without BQ123, BQ788, or cetrorelix ( $10^{-7}$  M), were added to the bottom chambers. ET-1 and GnRH elicited a sustained increase in migration (both \*,  $P < 0.0005$  vs. control). ET-1 effect was completely blocked by BQ788 but not by BQ123 and cetrorelix (both \*,  $P < 0.0005$  vs. control). GnRH-induced migration was completely counteracted by cetrorelix but not by the two ET-1 antagonists (both \*,  $P < 0.0005$  vs. control). Experiments were performed in triplicate. CTL, Control.





a role underlying the development of the specialized neuroendocrine cells as they migrate through nasal regions.

Maggi *et al.* (12) have shown that, during early embryonic life, ET-1 gene and protein, as well as endothelin-converting enzyme-1, are present in cells in the olfactory epithelium. From these data, together with our *in vitro* data, we speculate that, in the *in vivo* situation, ET-1 interacts with growth and differentiating factors not only to maintain a reservoir of GnRH-secreting neural cells but also to stimulate cell migration and a fully activated phenotype. Therefore, ET-1 could play a role in both guiding GnRH-secreting human neurons during their migration and orchestrating their subsequent differentiation.

During early embryogenesis, brain areas that undergo rapid neurogenic development and migration of cells through a differentiating matrix require very high energy for nutrients and the disposal of waste products. These requirements are best met by a rich blood supply. These needs constitute a possible trigger for the development of an elaborate “cellulo-vascular bridge” from the placode epithelium across the nasal septum and into the ventromedial forebrain (48). A close association between these angiogenic mechanisms and migration of GnRH neurons has been reported in embryonic mice, in early stage human embryos, and in those fetuses affected by Kallmann’s syndrome (48). Angiogenesis is an important early event not only in normal development but also in tumor progression, beginning in premalignant lesions (49). The endothelin system represents one of the most studied growth factor families that has been involved in modulating angiogenesis (50). Moreover, a close association between the loss of ETB receptor mRNA expression and the onset of a metastatic phenotype of neuroblastoma tumors, strictly associated with the disease progression, has been described previously (51). The blunted migration observed through specific ETB receptor antagonism in a human-derived neuroblastoma cell line suggested the possible role of ETB receptor activation in neoplastic differentiation. We thus hypothesize that ETB receptor signaling may be required in *in vivo* conditions to maintain a mature neuronal differentiation. Additional studies are needed to clarify whether the loss of ETB receptor expression during development can represent one of the underlying molecular mechanisms for both the hypogonadotropic hypogonadism as well as the onset of olfactory-derived tumors.

### Acknowledgments

We thank Prof. Vieri Boddi for his helpful supervision in statistical analysis.

Received January 14, 2005. Accepted June 15, 2005.

Address all correspondence and requests for reprints to: Gabriella B. Vannelli, Department of Anatomy Histology and Forensic Medicine, University of Florence, School of Medicine, V. le Morgagni 85, I-50134 Florence, Italy. E-mail: vannelli@unifi.it.

This work was supported by grants from the Ministero dell’Istruzione, dell’Università e della Ricerca, Telethon (number E523), and the University of Florence.

### References

- Schwanzel-Fukuda M 1999 Origin and migration of luteinizing hormone-releasing hormone neurons in mammals. *Microsc Res Tech* 44:2–10
- Wray S 2001 Development of luteinizing hormone releasing hormone neurones. *J Neuroendocrinol* 13:3–11
- MacColl G, Quinton R, Bouloux PM 2002 GnRH neuronal development: insights into hypogonadotropic hypogonadism. *Trends Endocrinol Metab* 13:112–118
- Yanagisawa M, Kurihara H, Kimura S, Tomobe Y, Kobayashi M, Mitsui Y, Yazaki Y, Goto K, Masaki T 1988 A novel potent vasoconstrictor peptide produced by vascular endothelial cells. *Nature* 332:411–415
- Inoue A, Yanagisawa M, Kimura S, Kasuya Y, Miyachi T, Goto K, Masaki T 1989 The human endothelin family: three structurally and pharmacologically distinct isopeptides predicted by three separate genes. *Proc Natl Acad Sci USA* 86:2863–2867
- Kedzierski RM, Yanagisawa M 2001 Endothelin system: the double-edged sword in health and disease. *Annu Rev Pharmacol Toxicol* 41:851–876
- Hempstead BL 2004 Sculpting organ innervation. *J Clin Invest* 113:811–813
- Schell DA, Murphy TC, Samson WK 1995 Endothelin modulation of prolactin secretion. In: Baldi E, Maggi M, Cameron IT, Dunn MJ, eds. *Endothelins in endocrinology: new advances*. Rome: Ares-Serono Symposia Publications; 145–151
- Kohzuki M, Chai SY, Paxinos G, Karavas A, Casley DJ, Johnston CI, Mendelsohn FA 1991 Localization and characterization of endothelin receptor binding sites in the rat brain visualized by *in vitro* autoradiography. *Neuroscience* 42:245–260
- Moretto M, Lopez FJ, Negro-Vilar A 1993 Endothelin-3 stimulates luteinizing hormone-releasing hormone (LHRH) secretion from LHRH neurons by a prostaglandin-dependent mechanism. *Endocrinology* 132:789–794
- Krsmanovic LZ, Stojkolovic SS, Balla T, Al-Damluji S, Weiner RI, Catt KJ 1991 Receptors and neurosecretory actions of endothelin in hypothalamic neurons. *Proc Natl Acad Sci USA* 88:11124–11128
- Maggi M, Barni T, Fantoni G, Mancina R, Pupilli C, Luconi M, Crescioli C, Serio M, Vannelli GB 2000 Expression and biological effects of endothelin-1 in human gonadotropin-releasing hormone-secreting neurons. *J Clin Endocrinol Metab* 85:1658–1665
- Kurihara Y, Kurihara H, Suzuki H, Kodama T, Maemura K, Nagai R, Oda H, Kuwaki T, Cao WH, Kamada N, Jishage K, Ouchi Y, Azuma S, Toyoda Y, Ishikawa T, Kumada M, Yazaki Y 1994 Elevated blood pressure and craniofacial abnormalities in mice deficient in endothelin-1. *Nature* 368:703–710
- Kurihara Y, Kurihara H, Oda H, Maemura K, Nagai R, Ishikawa T, Yazaki Y 1995 Aortic arch malformations and ventricular septal defect in mice deficient in endothelin-1. *J Clin Invest* 96:293–300
- Clouthier DE, Hosoda K, Richardson JA, Williams SC, Yanagisawa H, Kuwaki T, Kumada M, Hammer RE, Yanagisawa M 1998 Cranial and cardiac neural crest defects in endothelin-A receptor-deficient mice. *Development* 125:813–824
- Yanagisawa H, Yanagisawa M, Kapur RP, Richardson JA, Williams SC, Clouthier DE, de Wit D, Emoto N, Hammer RE 1998 Dual genetic pathways of endothelin-mediated intercellular signaling revealed by targeted disruption of endothelin converting enzyme-1 gene. *Development* 125:825–836
- Baynash AG, Hosoda K, Giaid A, Richardson JA, Emoto N, Hammer RE, Yanagisawa M 1994 Interaction of endothelin-3 with endothelin-B receptor is essential for development of epidermal melanocytes and enteric neurons. *Cell* 79:1277–1285
- Hosoda K, Hammer RE, Richardson JA, Baynash AG, Cheung JC, Giaid A, Yanagisawa M 1994 Targeted and natural (piebald-lethal) mutations of endothelin-B receptor gene produce megacolon associated with spotted coat color in mice. *Cell* 79:1267–1276
- Robertson K, Mason I, Hall S 1997 Hirschsprung’s disease: genetic mutations in mice and men. *Gut* 41:436–441
- McCallion AS, Chakravarti A 2001 EDNRB/EDN3 and Hirschsprung disease type II. *Pigment Cell Res* 14:161–169
- McCallion AS, Stames E, Conlon RA, Chakravarti A 2003 Phenotype variation in two-locus mouse models of Hirschsprung disease: tissue-specific interaction between Ret and EdnrB. *Proc Natl Acad Sci USA* 100:1826–1831
- Von Boyen GB, Krammer HM, Suss A, Dembowski C, Ehrenreich H, Wedel T 2002 Abnormalities of the enteric nervous system in heterozygous endothelin B receptor deficient (spotting lethal) rats resembling intestinal neuronal dysplasia. *Gut* 51:414–419
- Hou L, Pavan WJ, Shin MK, Arnheiter H 2004 Cell-autonomous and cell non-autonomous signaling through endothelin receptor B during melanocyte development. *Development* 131:3239–3247
- Carrasquillo MM, McCallion AS, Puffenberger EG, Kashuk CS, Nouri N, Chakravarti A 2002 Genome-wide association study and mouse model identify interaction between RET and EDNRB pathways in Hirschsprung disease. *Nat Genet* 32:237–244
- Barlow A, de Graaff E, Pachnis V 2003 Enteric nervous system progenitors are coordinately controlled by the G protein-coupled receptor EDNRB and the receptor tyrosine kinase RET. *Neuron* 40:905–916
- Kruger GM, Mosher JT, Tsai YH, Yeager KJ, Iwashita T, Garipey CE, Morrison SJ 2003 Temporally distinct requirements for endothelin receptor B in the generation and migration of gut neural crest stem cells. *Neuron* 40:917–929
- Romanelli RG, Barni T, Maggi M, Luconi M, Failli P, Pezzatini A, Pelo E,

- Torricelli F, Crescioli C, Ferruzzi P, Salerno R, Marini M, Rotella CM, Vannelli GB 2004 Expression and function of gonadotropin-releasing hormone (GnRH) receptor in human olfactory GnRH-secreting neurons: an autocrine GnRH loop underlies neuronal migration. *J Biol Chem* 279:117–126
28. Vannelli GB, Ensoli F, Zonefrati R, Kubota Y, Arcangeli A, Becchetti A, Camici G, Barni T, Thiele CJ, Balboni GC 1995 Neuroblast long-term cell cultures from human fetal olfactory epithelium respond to odors. *J Neurosci* 15:4382–4394
  29. Barni T, Maggi M, Fantoni G, Granchi S, Mancina R, Gulisano M, Marra F, Macorsini E, Luconi M, Rotella CM, Serio M, Balboni GC, Vannelli GB 1999 Sex steroids and odorants modulate gonadotropin-releasing hormone secretion in primary cultures of human olfactory cells. *J Clin Endocrinol Metab* 84:4266–4273
  30. Florio P, Vannelli GB, Luisi S, Barni T, Zonefrati R, Falaschi C, Bifulco G, Genazzani AR, Petraglia F 2000 Human GnRH-secreting cultured neurons express activin  $\beta$ A subunit mRNA and secrete dimeric activin A. *Eur J Endocrinol* 143:133–138
  31. Gonzalez-Martinez D, Kim SH, Hu Y, Guimond S, Schofield J, Winyard P, Vannelli GB, Turnbull J, Bouloux PM 2004 Anosmin-1 modulates fibroblast growth factor receptor 1 signaling in human gonadotropin-releasing hormone olfactory neuroblasts through a heparan sulfate-dependent mechanism. *J Neurosci* 24:10384–10392
  32. Radovick S, Wray S, Lee E, Nicols DK, Nakayama Y, Weintraub BD, Westphal H, Cutler Jr GB, Wondisford FE 1991 Migratory arrest of gonadotropin-releasing hormone neurons in transgenic mice. *Proc Natl Acad Sci USA* 88:3402–3406
  33. Ciccarone V, Spengler BA, Meyers MB, Biedler JL, Ross RA 1989 Phenotypic diversification in human neuroblastoma cells: expression of distinct neural crest lineages. *Cancer Res* 49:219–225
  34. Ensoli F, Fiorelli V, DeCristofaro M, Santini Muratori D, Novi A, Vannelli GB, Thiele CJ, Luzi G, Aiuti F 1999 Inflammatory cytokines and HIV-1-associated neurodegeneration: oncostatin-M produced by mononuclear cells from HIV-1-infected individuals induces apoptosis of primary neurons. *J Immunol* 162:6268–6277
  35. Encinas M, Iglesias M, Liu Y, Wang H, Muhaisen A, Cena V, Gallego C, Comella JX 2000 Sequential treatment of SH-SY5Y cells with retinoic acid and brain-derived neurotrophic factor gives rise to fully differentiated, neurotrophic factor-dependent, human neuron-like cells. *J Neurochem* 75:991–1003
  36. Vignozzi L, Filippi S, Luconi M, Morelli A, Mancina R, Marini M, Vannelli GB, Granchi S, Orlando C, Gelmini S, Ledda F, Forti G, Maggi M 2004 Oxytocin receptor is expressed in the penis and mediates an estrogen-dependent smooth muscle contractility. *Endocrinology* 145:1823–1834
  37. Morbidelli L, Orlando C, Maggi CA, Ledda F, Ziche M 1995 Proliferation and migration of endothelial cells is promoted by endothelins via activation of ETB receptors. *Am J Physiol* 269:H686–H695
  38. Granchi S, Vannelli GB, Vignozzi L, Crescioli C, Ferruzzi P, Mancina R, Vinci MC, Forti G, Filippi S, Luconi M, Ledda F, Maggi M 2002 Expression and regulation of endothelin-1 and its receptor in human penile smooth muscle cells. *Mol Hum Reprod* 8:1053–1064
  39. Filippi S, Morelli A, Vignozzi L, Vannelli GB, Marini M, Ferruzzi P, Mancina R, Crescioli C, Mondaini N, Forti G, Ledda F, Maggi M 2005 Oxytocin mediates the estrogen-dependent contractile activity of endothelin-1 in human and rabbit epididymis. *Endocrinology* 146:3506–3517
  40. De Lean A, Munson PJ, Rodbard D 1978 Simultaneous analysis of families of sigmoidal curves: application to bioassay, radioligand assay, and physiological dose-response curves. *Am J Physiol* 235:E97–E102
  41. Allen MP, Linseman DA, Udo H, Xu M, Schaack JB, Varnum B, Kandel ER, Heidenreich KA, Wierman ME 2002 Novel mechanism for gonadotropin-releasing hormone neuronal migration involving Gas6/Ark signaling to p38 mitogen-activated protein kinase. *Mol Cell Biol* 22:599–613
  42. Giacobini P, Giampietro C, Fioretto M, Maggi R, Carboni A, Perroteau I, Fasolo A 2002 Hepatocyte growth factor/scatter factor facilitates migration of GN-11 immortalized LHRH neurons. *Endocrinology* 143:3306–3315
  43. Graziadei PPC 1973 Cell dynamics in the olfactory mucosa. *Tissue Cell* 5:113–131
  44. Calof AL, Chikaraishi DM 1989 Analysis of neurogenesis in a mammalian neuroepithelium: proliferation and differentiation of an olfactory neuron precursor in vitro. *Neuron* 3:115–127
  45. Kondo T, Raff M 2000 Oligodendrocyte precursor cells reprogrammed to become multipotential CNS stem cells. *Science* 289:1754–1757
  46. Le Douarin NM, Dupin E 2003 Multipotentiality of the neural crest. *Curr Opin Genet Dev* 13:529–536
  47. Le Douarin NM, Creuzet S, Couly G, Dupin E 2004 Neural crest cell plasticity and its limits. *Development* 131:4637–4650
  48. Schwanzel-Fukuda M, Pfaff DW 2002 Angiogenesis in association with the migration of gonadotropic hormone-releasing hormone (GnRH) systems in embryonic mice, early human embryos and in a fetus with Kallmann's syndrome. *Prog Brain Res* 141:59–77
  49. Hanahan D, Weinberg RA 2000 The hallmarks of cancer. *Cell* 100:57–70
  50. Bagnato A, Spinella F 2003 Emerging role of endothelin-1 in tumor angiogenesis. *Trends Endocrinol Metab* 14:44–50
  51. Berry P, Burchill S 2002 Endothelins may modulate invasion and proliferation of Ewing's sarcoma and neuroblastoma. *Clin Sci (Lond)* 103:322S–326S

*Endocrinology* is published monthly by The Endocrine Society (<http://www.endo-society.org>), the foremost professional society serving the endocrine community.